

Resurrecting No-Scale Supergravity Phenomenology

John Ellis¹, Azar Mustafayev² and Keith A. Olive²

¹*TH Division, PH Department, CERN, CH-1211 Geneva 23, Switzerland*

²*William I. Fine Theoretical Physics Institute,
University of Minnesota, Minneapolis, MN 55455, USA*

Abstract

In the context of phenomenological models in which the soft supersymmetry-breaking parameters of the MSSM become universal at some unification scale, M_{in} , above the GUT scale, M_{GUT} , it is possible that all the scalar mass parameters m_0 , the trilinear couplings A_0 and the bilinear Higgs coupling B_0 vanish simultaneously, as in no-scale supergravity. Using these no-scale inputs in a renormalization-group analysis of the minimal supersymmetric SU(5) GUT model, we pay careful attention to the matching of parameters at the GUT scale. We delineate the region of M_{in} , $m_{1/2}$ and $\tan\beta$ where the resurrection of no-scale supergravity is possible, taking due account of the relevant phenomenological constraints such as electroweak symmetry breaking, $m_h, b \rightarrow s\gamma$, the neutralino cold dark matter density $\Omega_\chi h^2$ and $g_\mu - 2$. No-scale supergravity survives in an L-shaped strip of parameter space, with one side having with one side having $m_{1/2} \gtrsim 200$ GeV, the second (orthogonal) side having $M_{in} \gtrsim 5 \times 10^{16}$ GeV. Depending on the relative signs and magnitudes of the GUT superpotential couplings, these may be connected to form a triangle whose third side is a hypotenuse at larger M_{in} , $m_{1/2}$ and $\tan\beta$, whose presence and location depend on the GUT superpotential parameters. We compare the prospects for detecting sparticles at the LHC in no-scale supergravity with those in the CMSSM and the NUHM.

1 Introduction

Many of the uncertainties in the low-energy phenomenology of supersymmetry are associated with the pattern of supersymmetry breaking. Phenomenologists usually take a *bottom-up* approach, *e.g.*, postulating some form of universality for the soft supersymmetry-breaking (SSB) parameters m_0 , $m_{1/2}$ and A_0 , motivated by the observed suppression of flavour-changing neutral interactions [1]. This suggests that, before renormalization, the SSB scalar masses are (approximately) universal for squarks and sleptons in different generations that have the same electroweak quantum numbers [2]. Grand Unified Theories (GUTs) such as SU(5) further suggest universality between the the SSB scalar masses for squarks and sleptons in the same GUT multiplet, *e.g.*, the left-handed sleptons and the right-handed charge- $(-1/3)$ squarks in a fiveplet of SU(5). Universality between the the SSB scalar masses in the fiveplet and tenplet of SU(5) might be motivated by a larger GUT such as SO(10), but universality with the SSB masses of the Standard Model Higgs multiplets would require some principle beyond GUTs. Nevertheless, this extended universality is often postulated, particularly at the GUT scale in the framework of the constrained MSSM (CMSSM) [3–9], though models with non-universal Higgs masses (NUHM) are also often studied [9–11]. All of these models are usually analyzed assuming that the gravitino is heavy and the lightest supersymmetric particle (LSP) is the lightest neutralino χ [12].

On the other hand, taking a *top-down* point of view, supersymmetry breaking presumably originates from the spontaneous breaking of local supersymmetry via the super-Higgs mechanism in $N = 1$ supergravity [13–15]. Therefore the pattern of supersymmetry breaking is linked to the form of the effective supergravity theory that, in turn, presumably originates from some form of superstring theory. One of the most popular hypotheses is that of minimal supergravity (mSUGRA) in which the Kähler potential K characterizing the kinetic terms of the chiral supermultiplets Φ_i has the simple form $K = \sum_i |\Phi_i|^2$ [16]. In this case, universality of the m_0 and A_0 would be automatic and there would, in addition, be a relation for the soft bilinear Higgs coupling $B_0 = A_0 - m_0$ and the gravitino mass would be fixed: $m_{3/2} = m_0$ [16, 17]. The first of these constraints can be regarded as fixing, via the electroweak vacuum conditions [18], $\tan\beta$ as a function of $m_{1/2}$, m_0 and A_0 , and the latter condition implies that the gravitino is the LSP in extensive regions of parameter space. Hence mSUGRA is not equivalent to the CMSSM.

Other forms of effective supergravity theory have also been suggested, and the possibility we study here is no-scale supergravity [19], in which $m_0 = A_0 = B_0 = 0$ before renormalization¹. The Kähler potential for the simplest form of no-scale supergravity for a single chiral supermultiplet T is $K = -3\ln(T + T^\dagger)$, and the simplest form for many additional chiral supermultiplets Φ_i is $K = -3\ln(T + T^\dagger - \sum_i |\Phi_i|^2)$. Many other forms of Kähler potential also have the no-scale property, notably those derived as effective theories from string models [20], where T can be regarded as a prototype modulus field. We note that the no-scale boundary conditions also arise in models of gaugino mediation [21] considered in the context of brane-world models.

However, for many years no-scale supergravity phenomenology has been disfavoured,

¹The gravitino is not expected to be the LSP in such no-scale models.

because data seemed to disfavour small values of m_0 and specifically $m_0 = 0$. For example, in [22] it was concluded that a framework with unified gaugino masses and $m_0 = 0$ at the GUT scale would be possible only for a very restricted range of $\tan\beta \sim 8$ ². It was also suggested [22] that no-scale supergravity could be rescued over a larger range of $\tan\beta$ if the no-scale boundary condition applied at the Planck scale. Indeed, it was recognized in Ref. [24] that the problem of a stau LSP can be alleviated when the unification scale is raised sufficiently above the GUT scale, leaving the possibility open for a bino LSP as dark matter. The superpartner spectrum found in gaugino mediation models with a high unification scale was discussed in Ref. [25].

We have recently studied [26] how the parameter space of the CMSSM is modified if SSB scalar mass universality is imposed at some scale $M_{in} > M_{GUT}$. Specifically, we studied the minimal SU(5) GUT model [27] with m_0 defined at some scale $M_{GUT} \leq M_{in} \leq \overline{M}_P \equiv M_P/\sqrt{2\pi} \sim 2.4 \times 10^{18}$ GeV³. The regions of the $(m_{1/2}, m_0)$ plane favoured by the available phenomenological constraints such as the density of neutralino dark matter $\Omega_\chi h^2$ change substantially with M_{in} and we confirmed, in particular, the previous observations [22, 24] that the option $m_0 = 0$ could be permitted under some circumstances. This study did not, however, apply directly to no-scale models, since the conditions $A_0 = B_0 = 0$ were not imposed at M_{in} .

In this paper we study systematically the consequences of applying the full no-scale conditions $m_0 = A_0 = B_0 = 0$ at some common scale $M_{in} > M_{GUT}$ in the framework of the simplest SU(5) GUT. Assuming that the gravitino is heavy, the only relevant supersymmetry-breaking parameter in this model is $m_{1/2}$. However, in principle, even the simplest SU(5) also has two GUT superpotential parameters λ, λ' [26], whose values influence the allowed region in the no-scale $(m_{1/2}, M_{in})$ plane. We find here that the region of this plane allowed by all the phenomenological constraints is a narrow WMAP-compatible L-shaped strip with a rounded corner. Its near-vertical part has $m_{1/2} \gtrsim 200$ GeV, and the near-horizontal second side has $M_{in} \gtrsim 5 \times 10^{16}$ GeV. Depending on the magnitudes and relative signs of the GUT superpotential parameters, the L shape may become a triangle whose third side (the hypotenuse) connects the ends of the L shape though larger values of M_{in} , $m_{1/2}$ and $\tan\beta$. The triangle contracts to a ‘blob’ and then disappears as $-\lambda$ increases, for any fixed value of $\lambda' > 0$. Based on this analysis, we then discuss the prospects for detecting supersymmetry at the LHC within the no-scale supergravity framework.

2 The Minimal SU(5) GUT Superpotential and RGEs

In order to discuss the evolution of model parameters above the GUT scale, we adopt the minimal SU(5) GUT model [27] with the conventional assignments of matter superfields to $\mathbf{\bar{5}}$ and $\mathbf{10}$ representations. In this model, SU(5) is broken down to the Standard Model gauge group by a single adjoint Higgs multiplet $\hat{\Sigma}(\mathbf{24})$, and the renormalizable part of the

²One can remove the unpleasant stau LSP feature by considering non-universal gaugino masses arising from a restricted gauge symmetry on the hidden brane [23].

³For a recent review of this sample model and its compatibility with experiment, see [28].

superpotential for this and the two five-dimensional SU(5) representations $\hat{\mathcal{H}}_1(\bar{\mathbf{5}})$ and $\hat{\mathcal{H}}_2(\mathbf{5})$ is

$$W_H = \mu_\Sigma \text{Tr} \hat{\Sigma}^2 + \frac{1}{6} \lambda' \text{Tr} \hat{\Sigma}^3 + \mu_H \hat{\mathcal{H}}_{1\alpha} \hat{\mathcal{H}}_2^\alpha + \lambda \hat{\mathcal{H}}_{1\alpha} \hat{\Sigma}_\beta^\alpha \hat{\mathcal{H}}_2^\beta, \quad (1)$$

where Greek letters denote SU(5) indices. The corresponding soft SUSY-breaking lagrangian terms are

$$\begin{aligned} \mathcal{L}_{soft} \ni & -m_{\mathcal{H}_1}^2 |\mathcal{H}_1|^2 - m_{\mathcal{H}_2}^2 |\mathcal{H}_2|^2 - m_\Sigma^2 \text{Tr}(\Sigma^\dagger \Sigma) \\ & - \left[B_\Sigma \mu_\Sigma \text{Tr} \Sigma^2 + \frac{1}{6} A_{\lambda'} \lambda' \text{Tr} \Sigma^3 + B_H \mu_H \mathcal{H}_{1\alpha} \mathcal{H}_2^\alpha + A_\lambda \lambda \mathcal{H}_{1\alpha} \Sigma_\beta^\alpha \mathcal{H}_2^\beta + h.c. \right]. \end{aligned} \quad (2)$$

In addition, \mathcal{L}_{soft} also contains mass terms for the gaugino fields (M_5) for the first- and second-generation fermionic fields ($m_{\bar{\mathbf{5}},1}$ and $m_{\mathbf{10},1}$) and their third-generation counterparts ($m_{\bar{\mathbf{5}}}$ and $m_{\mathbf{10}}$), as well as trilinear scalar couplings ($A_{\bar{\mathbf{5}}}$ and $A_{\mathbf{10}}$). Note that μ_H and μ_Σ are of $\mathcal{O}(M_{GUT})$, while the rest of the soft parameters are of $\mathcal{O}(M_{weak})$.

The minimal SU(5) GUT model assumes universality of corresponding soft SUSY-breaking terms and is completely specified the following set of parameters

$$m_0, m_{1/2}, A_0, B_0, M_{in}, \lambda, \lambda', \text{sgn}(\mu). \quad (3)$$

In its no-scale incarnation, we impose at the scale M_{in}

$$\begin{aligned} m_{\bar{\mathbf{5}},1} = m_{\mathbf{10},1} = m_{\bar{\mathbf{5}}} = m_{\mathbf{10}} = m_{\mathcal{H}_1} = m_{\mathcal{H}_2} = m_\Sigma & \equiv m_0 = 0, \\ A_{\bar{\mathbf{5}}} = A_{\mathbf{10}} = A_\lambda = A_{\lambda'} & \equiv A_0 = 0, \\ B_\Sigma = B_H & \equiv B_0 = 0, \\ M_5 & \equiv m_{1/2}. \end{aligned} \quad (4)$$

These soft parameters along with gauge and Yukawa couplings are evolved between M_{in} and M_{GUT} using the SU(5) RGEs given in Ref. [27].

The renormalization-group equations (RGEs) for the third-generation matter Yukawa couplings $h_{\bar{\mathbf{5}}}$ and $h_{\mathbf{10}}$ between M_{in} and M_{GUT} are:

$$\frac{dh_{\bar{\mathbf{5}}}}{dt} = \frac{h_{\bar{\mathbf{5}}}}{16\pi^2} \left[5h_{\bar{\mathbf{5}}}^2 + 48h_{\mathbf{10}}^2 + \frac{24}{5}\lambda^2 - \frac{84}{5}g_5^2 \right], \quad (5)$$

$$\frac{dh_{\mathbf{10}}}{dt} = \frac{h_{\mathbf{10}}}{16\pi^2} \left[144h_{\mathbf{10}}^2 + 2h_{\bar{\mathbf{5}}}^2 + \frac{24}{5}\lambda^2 - \frac{96}{5}g_5^2 \right], \quad (6)$$

where g_5 is the SU(5) gauge coupling above the GUT scale. We note that the Yukawa coupling λ , but not λ' , contributes directly to the RGEs for $h_{\bar{\mathbf{5}}}$ and $h_{\mathbf{10}}$. Likewise, the RGEs for the most relevant trilinear parameters between M_{in} and M_{GUT} also involve λ but not λ' :

$$\frac{dA_{\bar{\mathbf{5}}}}{dt} = \frac{1}{8\pi^2} \left[5A_{\bar{\mathbf{5}}}h_{\bar{\mathbf{5}}}^2 + 48A_{\mathbf{10}}h_{\mathbf{10}}^2 + \frac{24}{5}A_\lambda\lambda^2 - \frac{84}{5}g_5^2M_5 \right], \quad (7)$$

$$\frac{dA_{\mathbf{10}}}{dt} = \frac{1}{8\pi^2} \left[2A_{\bar{\mathbf{5}}}h_{\bar{\mathbf{5}}}^2 + 144A_{\mathbf{10}}h_{\mathbf{10}}^2 + \frac{24}{5}A_\lambda\lambda^2 - \frac{96}{5}g_5^2M_5 \right], \quad (8)$$

as do the RGEs for the soft supersymmetry-breaking squared scalar masses of the electroweak Higgs multiplets. The appearances of λ in these RGEs imply that our results are more sensitive to this coupling than to λ' , as we discuss later.

The matching to MSSM parameters is done at M_{GUT} as following:

$$\begin{aligned}
g_1 = g_2 = g_3 = g_5, & \quad h_t = 4h_{\mathbf{10}}, \\
M_1 = M_2 = M_3 = M_5, & \quad (h_b + h_\tau)/2 = h_{\overline{\mathbf{5}}}/\sqrt{2}, \\
A_t = A_{\mathbf{10}}, & \quad A_b = A_\tau = A_{\overline{\mathbf{5}}}, \\
m_{D_1}^2 = m_{L_1}^2 = m_{\overline{\mathbf{5}},1}^2, & \quad m_{Q_1}^2 = m_{U_1}^2 = m_{E_1}^2 = m_{\mathbf{10},1}^2, \\
m_{D_3}^2 = m_{L_3}^2 = m_{\overline{\mathbf{5}}}^2, & \quad m_{Q_3}^2 = m_{U_3}^2 = m_{E_3}^2 = m_{\mathbf{10}}^2, \\
m_{H_d}^2 = m_{\mathcal{H}_1}^2, & \quad m_{H_u}^2 = m_{\mathcal{H}_2}^2.
\end{aligned} \tag{9}$$

Below M_{GUT} , the standard MSSM RGEs [29] are used to obtain values of soft parameters at lower scales ⁴. As mentioned in Ref [26], we do not impose the condition of exact $b - \tau$ yukawa unification at M_{GUT} , since there could be non-renormalizable operators in SU(5) that are necessary to correct the poor Yukawa relations for the lighter families.

The Higgs bilinear superpotential μ terms and the soft supersymmetry-breaking B terms decouple from the rest of RGEs. This enables one to use the EWSB minimization conditions [18] to trade $\tan\beta$ for B_0 and predict μ^2 as a function of soft parameters and B_0 . In the true no-scale framework, the B terms must also vanish at M_{in} , as seen in (4) ⁵. The B terms are then evolved down to M_{GUT} using the following RGEs:

$$\begin{aligned}
\frac{dB_H}{dt} &= \frac{1}{8\pi^2} \left[48A_{\mathbf{10}}h_{\mathbf{10}}^2 + 2A_{\overline{\mathbf{5}}}h_{\overline{\mathbf{5}}}^2 + \frac{48}{5}A_\lambda\lambda^2 - \frac{48}{5}M_5g_5^2 \right], \\
\frac{dB_\Sigma}{dt} &= \frac{1}{8\pi^2} \left[2A_\lambda\lambda^2 + \frac{21}{10}A_{\lambda'}\lambda'^2 - 20M_5g_5^2 \right].
\end{aligned} \tag{10}$$

In this case, $\tan\beta$ is fixed as a function of the other parameters by the electroweak vacuum conditions, and the free parameters of the model are simply

$$m_{1/2}, M_{in}, \lambda, \lambda' \tag{11}$$

and, motivated by $g_\mu - 2$ measurements [32, 33], we choose $\mu > 0$.

It was observed in [17] that the value of the MSSM parameter B at the GUT scale has a strong influence in low-energy parameters, particularly $\tan\beta$. Accordingly, we pay close attention to the boundary condition for B that matches correctly the GUT renormalization downwards from M_{in} , where we assume $B_0 = A_0 = m_0 = 0$, to the continuing MSSM RGE analysis down to the electroweak scale. This matching has been studied carefully in [34], and we present below the major steps of the derivation using our notation.

⁴For the MSSM RGEs, we use the convention of [30] which have opposite signs for all trilinear and bilinear SSB terms relative to those in [29].

⁵As we will see later, this condition imposes very strong constraints on the parameter space and the allowed dark-matter annihilation mechanism, as compared to minimal SU(5) with vanishing m_0 and A_0 , but arbitrary B_Σ , B_H , that was discussed for example in Ref. [26, 31].

The adjoint Higgs multiplet $\hat{\Sigma}$ can be represented by a traceless matrix:

$$\hat{\Sigma}_\beta^\alpha = \sqrt{2}\hat{\Sigma}_r(T_r)_\beta^\alpha, \quad (12)$$

where the T_r ($r = 1..24$) are SU(5) generators with $\text{Tr}(T_r T_s) = \delta_{rs}/2$, The breaking $SU(5) \rightarrow SU(3)_c \times SU(2)_L \times U(1)_Y$ arises from the Standard-Model singlet component $\hat{\Sigma}_{24}$, that develops a vev of $\mathcal{O}(M_{GUT})$, $\langle \hat{\Sigma} \rangle = \langle \hat{\Sigma}_{24} \rangle \text{diag}(2, 2, 2, -3, -3)$. The latter can be decomposed as

$$\langle \hat{\Sigma}_{24} \rangle = \langle \Sigma_{24} \rangle + \theta^2 \langle \mathcal{F}_{24} \rangle, \quad (13)$$

where Σ_{24} and \mathcal{F}_{24} are, respectively, the scalar and auxiliary field components of superfield $\hat{\Sigma}_{24}$. The auxiliary component is determined from the superpotential (1) to be

$$\mathcal{F}_{24}^\dagger = \left(\frac{\partial W_H}{\partial \hat{\Sigma}_{24}} \right)_{\hat{\Sigma}=\Sigma} = 2\mu_\Sigma \Sigma_{24} - \frac{1}{2\sqrt{30}} \lambda' \Sigma_{24}^2. \quad (14)$$

We can find both the scalar and auxiliary component vevs by minimizing the relevant part of the scalar potential that breaks SU(5)

$$V_{\Sigma_{24}} = |\mathcal{F}_{24}|^2 + \tilde{V}_{\Sigma_{24}}, \quad (15)$$

where $\tilde{V}_{\Sigma_{24}}$ is a subset of soft supersymmetry-breaking terms (2) that contains only Σ_{24} fields. Using $\delta \equiv (M_{SUSY}/M_{GUT})$ as an expansion parameter, we can find perturbative solutions of the form

$$\begin{aligned} \langle \Sigma_{24} \rangle &= v_{24} + \delta v_{24} + \delta^2 v_{24} + \mathcal{O}\left(\frac{M_{SUSY}^3}{M_{GUT}^2}\right) \\ \langle \mathcal{F}_{24} \rangle &= 0 + F_{24} + \delta F_{24} + \mathcal{O}\left(\frac{M_{SUSY}^3}{M_{GUT}}\right). \end{aligned} \quad (16)$$

The first terms on the right-hand sides of (16) correspond to the case of exact supersymmetry: since $\langle \hat{\Sigma}_{24} \rangle$ breaks only SU(5) and not supersymmetry, it vanishes for the auxiliary field. For the scalar component vev we get the familiar expression $v_{24} = 2\sqrt{30}\mu_\Sigma/\lambda'$. The subsequent terms represent corrections induced by the presence of the soft terms [35].

The MSSM Higgs bilinears μ and B can be expressed in terms of SU(5) parameters as

$$\begin{aligned} \mu &= \mu_H - \frac{3}{\sqrt{30}} \lambda \langle \Sigma_{24} \rangle, \\ B\mu &= B_H \mu_H - \frac{3}{\sqrt{30}} \lambda (A_\lambda \langle \Sigma_{24} \rangle + \langle \mathcal{F}_{24} \rangle). \end{aligned} \quad (17)$$

Using the expansions (16) and eliminating μ_H , we obtain the following expression for the MSSM parameter B in terms of the SU(5) quantities and μ :

$$B = B_H - \frac{6\lambda}{\mu\lambda'} [(B_\Sigma - A_\lambda)(2B_\Sigma - A_\lambda) + m_\Sigma^2], \quad (18)$$

where we have used the fact that the combination $\Delta \equiv B_H - A_\lambda - B_\Sigma - A_{\lambda'}$ is a RGE invariant (at one loop) and therefore remains zero at all scales. To help understand the behaviour of this matching condition we also list the relevant RGEs for $A_{\lambda'}$ and m_Σ^2 ,

$$\frac{dA_{\lambda'}}{dt} = \frac{1}{8\pi^2} \left[3\lambda^2 A_\lambda + \frac{63}{20}\lambda'^2 A_{\lambda'} - 30g_5^2 M_5 \right], \quad (19)$$

$$\frac{dm_\Sigma^2}{dt} = \frac{1}{8\pi^2} \left[\lambda^2 (m_{\mathcal{H}_1}^2 + m_{\mathcal{H}_2}^2 + m_\Sigma^2 + A_\lambda^2) + \frac{21}{20}\lambda'^2 (3m_\Sigma^2 + A_{\lambda'}^2) - 20g_5^2 M_5^2 \right]. \quad (20)$$

We note in passing that all the RGEs shown above involve just the squares of λ and λ' , and hence are insensitive to their signs. However, the relative sign of λ and λ' does enter into the matching conditions (17), with the consequences for phenomenology that we discuss in the next Section.

3 The $(m_{1/2}, M_{in})$ Plane of No-Scale Supergravity

We now discuss the $(m_{1/2}, M_{in})$ planes for the no-scale supergravity model with various values of λ and λ' shown in Figs. 1 and 2, where we limit ourselves to $M_{in} \leq \overline{M}_P$. These plots are for positive λ' and negative λ : it is easy to check that the results are independent of the *overall* sign of λ' and λ , but are sensitive to their *relative* sign. The plots in Figs. 1 and 2 are for the (more interesting) case in which λ' and λ have opposite signs, we discuss later the (less interesting) same-sign case. We recall that in all of the figures we have set $m_0 = A_0 = B_0 = 0$ and $\mu > 0$. We concentrate on values of $\lambda' \geq 1$ since on the one hand, as we discuss below, the values of λ allowed in no-scale models are typically $\ll \lambda'$ and, on the other hand, small values of λ are disfavoured by proton stability. We are able to find stable solutions of the RGEs for $\lambda' \lesssim 2.6$: the features seen in Figs. 1 and 2 persist up to the largest values of λ' that we have studied.

For RGE calculations we used the program `SSARD` [36], which allows the computation of sparticle spectrum on the basis of 2-loop RGE evolution for the MSSM [29] and 1-loop evolution for minimal SU(5) [27], and perform cross-checks with `ISAJET 7.80` [37] modified to include SU(5) running above M_{GUT} . We set soft parameters at M_{in} according to Eqs.(4) and perform matching between SU(5) and MSSM according to expressions (9,18) at the scale M_{GUT} . The location of the latter is determined dynamically as the scale where $g_1 = g_2$, and is approximately 1.5×10^{16} GeV. Throughout the paper we assume $m_t = 173.1$ GeV [38] and $m_b^{\overline{MS}}(m_b) = 4.2$ GeV [39].

In each plane of Figs. 1 and 2, we indicate by brown shading the region that is excluded because the LSP is the lighter stau $\tilde{\tau}_1$, and the region where we find no consistent solution of the RGEs is indicated by orange shading. Our treatment of $BR(b \rightarrow s\gamma)$ follows that in [40,41], and the region excluded at the 95% CL [42] is shaded green. The region favoured by $g_\mu - 2$ measurements [32,33] if the Standard Model contribution is calculated using low-energy e^+e^- data [43] is shaded pink, with the $\pm 1\text{-}\sigma$ contours shown as black dashed lines and the $\pm 2\text{-}\sigma$ contours shown as solid black lines. The LEP lower limit on the chargino mass [44] is shown as a thick black dashed line, and the experimental lower limit on m_h [45]

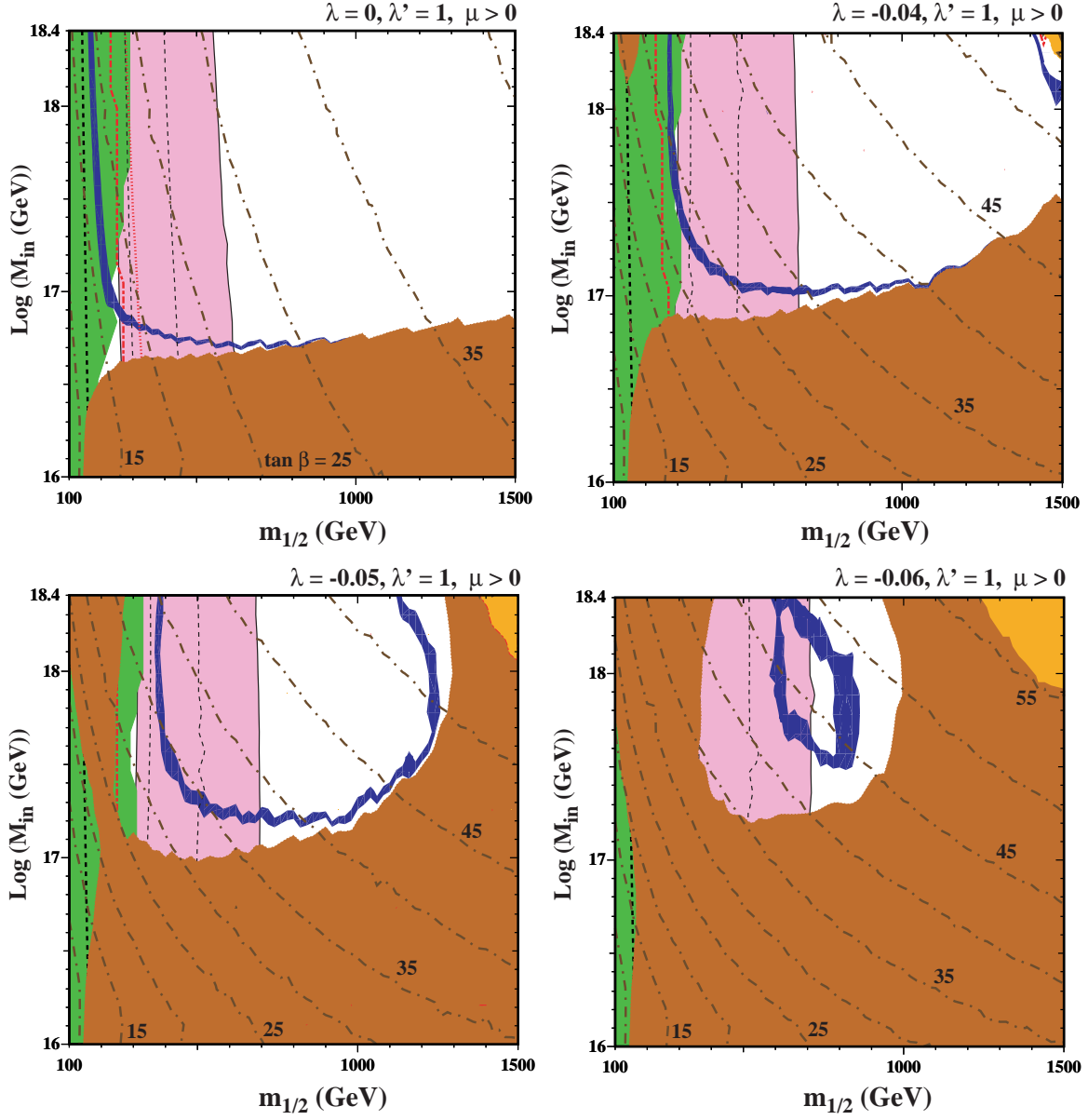


Figure 1: The $(m_{1/2}, M_{in})$ planes for the no-scale supergravity model with $\lambda' = 1$ and (a) $\lambda = 0$, (b) $\lambda = -0.04$, (c) $\lambda = -0.05$ and (d) $\lambda = -0.06$. The relic density $\Omega_\chi h^2$ is within the WMAP range in the blue strip. The pink region between the black dashed (solid) lines is allowed by $g_\mu - 2$ at the $1\text{-}\sigma$ ($2\text{-}\sigma$) level. The diagonal dark brown dash-dotted lines are contours of $\tan\beta$, as determined by the electroweak vacuum conditions. The brown and green colored regions are excluded by the requirements of a neutralino LSP, and by $b \rightarrow s\gamma$, respectively, and in the orange region we find no consistent solutions to the RGEs. Areas to the left of the thick black dashed and red dash-dotted lines are ruled out by LEP searches for charginos and the lightest MSSM Higgs, respectively. More details can be found in the text.

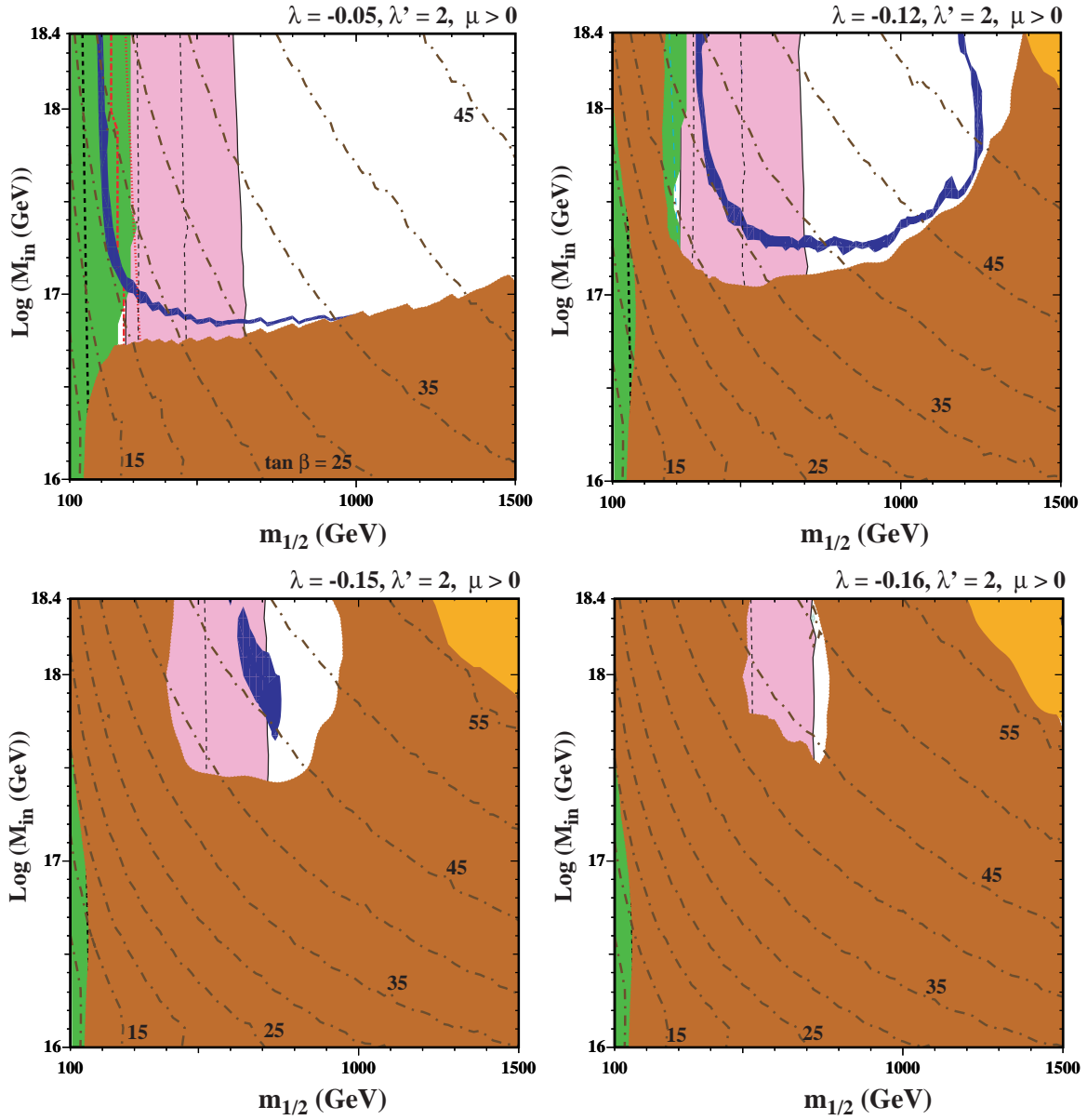


Figure 2: *Similar to Fig. 1, but for $\lambda' = 2$ and (a) $\lambda = -0.05$, (b) $\lambda = -0.12$, (c) $\lambda = -0.15$ and (d) $\lambda = -0.16$.*

is indicated as a red dash-dotted line. This shows the position of the 95% confidence-level lower limit obtained by combining the experimental likelihood from direct searches at LEP 2 and a global electroweak fit, convolved with the theoretical and parametric errors in m_h ⁶, which provides a more exact (and relaxed) interpretation of the nominal LEP Higgs limit of 114.4 GeV within the MSSM. In the models under study, the couplings of the lightest supersymmetric Higgs are very similar to those in the Standard Model, so the same nominal lower limit $m_h > 114.4$ GeV applies. However, the light Higgs mass is computed in terms of the model parameters using the `FeynHiggs 2.6.5` code [46], whose nominal results are assigned a theoretical error ~ 1.5 GeV in drawing the exclusion contour, moving it towards smaller $m_{1/2}$ by ~ 50 GeV ⁷. Finally, we use blue colour to indicate the regions where the neutralino relic density falls within the $2\text{-}\sigma$ WMAP range [47], $0.097 \leq \Omega_{CDM} h^2 \leq 0.122$.

The diagonal dark brown dash-dotted lines in Figs. 1 and 2 are contours of $\tan \beta$, rising in steps of 5 from left to right. The intercepts of the $\tan \beta$ contours on the $m_{1/2}$ axis are the same in all panels, *e.g.*, $\tan \beta = 15$ when $m_{1/2} \simeq 260$ GeV and $\tan \beta = 25$ when $m_{1/2} \simeq 700$ GeV, but the slopes of the contours depend on the no-scale parameters λ, λ' , rotating counter-clockwise as λ decreases for any fixed value of λ' . This behaviour arises because the value of $\tan \beta$ for any point on the plane is sensitively tied to the matching condition in Eq. (18). In Ref. [17], it was shown that GUT-scale value of the MSSM B parameter is almost always a monotonically-increasing function of $\tan \beta$ in the CMSSM. While its slope with respect to $\tan \beta$ is steep at low $\tan \beta$, it increases very little for $\tan \beta \gtrsim 10$. As a result, relatively small changes in the required value for B_{MGUT} could entail very large changes in $\tan \beta$.

From the RGEs of $A_{\lambda'}$, m_{Σ}^2 , B_H and B_{Σ} in Eqs. (10, 20) we can understand the qualitative behaviour of the $\tan \beta$ contours. Since our boundary conditions at M_{in} correspond to $A_0 = 0$ and $m_{\Sigma}^2 = 0$, the initial driving force in all of the relevant RGEs comes from the non-zero gaugino mass, M_5 , driving $A_{\lambda'}$, B_H , and B_{Σ} positive and driving the dominant term m_{Σ}^2 positive. As M_{in} is increased, the right-hand side of the matching condition (17) is driven higher (for $\lambda/\lambda' < 0$), resulting in a larger value for $\tan \beta$. Similarly, a larger value for $m_{1/2}$ (M_5) leads to a larger initial kick in the RGE evolution, which also increases the right-hand side of Eq. (17) and hence leads to higher $\tan \beta$. This is precisely the pattern we see in Figures 1 and 2. At very large M_{in} and/or $m_{1/2}$, $\tan \beta$ is pushed above 55, and soon thereafter we are not able to obtain solutions to the MSSM RGEs. This area is shaded orange. Furthermore, we see that as we increase $-\lambda$ (for fixed λ') we again increase the right-hand side of Eq. (17) and the $\tan \beta$ contours rotate counter-clockwise, so that we obtain higher $\tan \beta$ for any given choice of $(m_{1/2}, M_{in})$.

The $(m_{1/2}, M_{in})$ planes in Fig. 1 are for $\lambda' = 1$ and (a) $\lambda = 0$, (b) $\lambda = -0.04$, (c) $\lambda = -0.05$ and (d) $\lambda = -0.06$. We see that in the first two panels of Fig. 1 the WMAP-compatible region takes the form of a thin L-shaped strip in the $(m_{1/2}, M_{in})$ plane with a rounded corner: points above and to the right of the L have values of $\Omega_{\chi} h^2$ that are too large. In panel (a) for $\lambda = 0$, the near-horizontal part of the line is located at $M_{in} \sim 5 \times 10^{16}$ GeV and extends from $m_{1/2} \sim 200$ GeV to ~ 1000 GeV, larger values being excluded by the

⁶ We thank A. Read for providing the LEP CL_s values.

⁷The constraint that would be obtained with the nominal value $m_h = 114.4$ GeV is also shown, for comparison, as a dotted red line in the top left panels of Figs. 1 and 2.

requirement that the LSP not be charged, and we find that $\tan\beta \in (16, 30)$. All the base strip is compatible with the LEP chargino constraint, and with $b \rightarrow s\gamma$. However, only the portion with $m_{1/2} \gtrsim 300$ GeV is compatible with the LEP lower limit on m_h , taking into account the theoretical uncertainty in the `FeynHiggs` calculation of m_h , and the near-vertical part of the no-scale strip is always incompatible with the LEP Higgs constraint and (mostly) $b \rightarrow s\gamma$.

In panel (b) of Fig. 1 for $\lambda = -0.04$, the near-vertical part of the WMAP-compatible strip has moved to larger values of $m_{1/2} \sim 300$ GeV, and is now compatible with the LEP Higgs constraint and (mostly) the $b \rightarrow s\gamma$ constraint. Also, the values of M_{in} along the near-horizontal part of the allowed strip rise to $M_{in} \gtrsim 10^{17}$ GeV, values of $m_{1/2} \lesssim 1300$ GeV have a neutralino LSP, and $\tan\beta \lesssim 45$. We also note in the upper right corner of panel (b) of Fig. 1 the appearance of a portion of another WMAP-compatible strip at $\tan\beta > 50$.

Panel (c) of Fig. 1 for $\lambda = -0.05$ has a rather different appearance, but is in fact a natural continuation of the trends seen in the previous panels. In particular, the near-vertical part of the WMAP-compatible strip has moved to larger $m_{1/2} \sim 400$ GeV, and is compatible with both m_h and $b \rightarrow s\gamma$, and the near-horizontal part of the strip has risen to $M_{in} \sim 2 \times 10^{17}$ GeV. More dramatically, the WMAP-compatible strip now becomes a (rounded) triangle, with a hypotenuse connecting the previous two strips at relatively large $m_{1/2}$ and M_{in} and $\tan\beta \gtrsim 50$ (though the triangle closes only when $M_{in} > \overline{M_P}$), expanding the fragment of the hypotenuse visible in the upper right corner of panel (b) of Fig. 1. We emphasize that all the triangle has a neutralino LSP, and that the stau-LSP contour loops around the base and hypotenuse: the region within the triangle has too much dark matter.

Turning finally to panel (d) of Fig. 1 for $\lambda = -0.06$, we see that the triangle has contracted to an ‘doughnut’ with $m_{1/2} \in (600, 900)$ GeV, $M_{in} \in (3 \times 10^{17}, 3 \times 10^{18})$ GeV and $\tan\beta \in (42, 49)$, all of which is again compatible with the LEP Higgs constraint and $b \rightarrow s\gamma$, and sits partly in the region preferred by $g_\mu - 2$. Once more, the stau-LSP contour loops around the doughnut. As λ is dialed to more negative values the doughnut continues to shrink and eventually disappears for $\lambda \lesssim -0.07$.

A similar evolutionary pattern as λ decreases is seen in Fig. 2, where we fix $\lambda' = 2$. In panel (a) for $\lambda = -0.05$, the WMAP-compatible strip is again L-shaped, with a near-vertical part at $m_{1/2} \sim 200$ GeV that is incompatible with the Higgs constraint and $b \rightarrow s\gamma$, and a near-horizontal part at $M_{in} \sim 8 \times 10^{16}$ GeV that extends to $m_{1/2} \sim 1000$ GeV before the LSP ceases to be a neutralino. At $\lambda = -0.12$ the region allowed by the relic density has the same (rounded) triangular form as panel (c) of Fig. 1 (the triangle again closes only when $M_{in} > \overline{M_P}$). We see again the feature of the stau-LSP contour looping around the WMAP-compatible strip. In panel (c) for $\lambda = -0.15$ we see just a ‘blob’ with $m_{1/2} \in (500, 650)$ GeV and $M_{in} \in (5 \times 10^{17}, 3 \times 10^{18})$ GeV on the edge of the region preferred by $g_\mu - 2$. This remaining ‘blob’ disappears for larger $-\lambda$ as shown in panel (d) for $\lambda = -0.16$. Here, the area within the ‘window’ is phenomenologically allowed, though the relic density lies below the WMAP range.

So far, we have displayed the regions of no-scale parameter space allowed when λ and λ' have opposite signs. We now discuss the same-sign case, based on the examples shown in Fig. 3. As λ/λ' increases and becomes positive, the matching conditions (17, 18) drive the

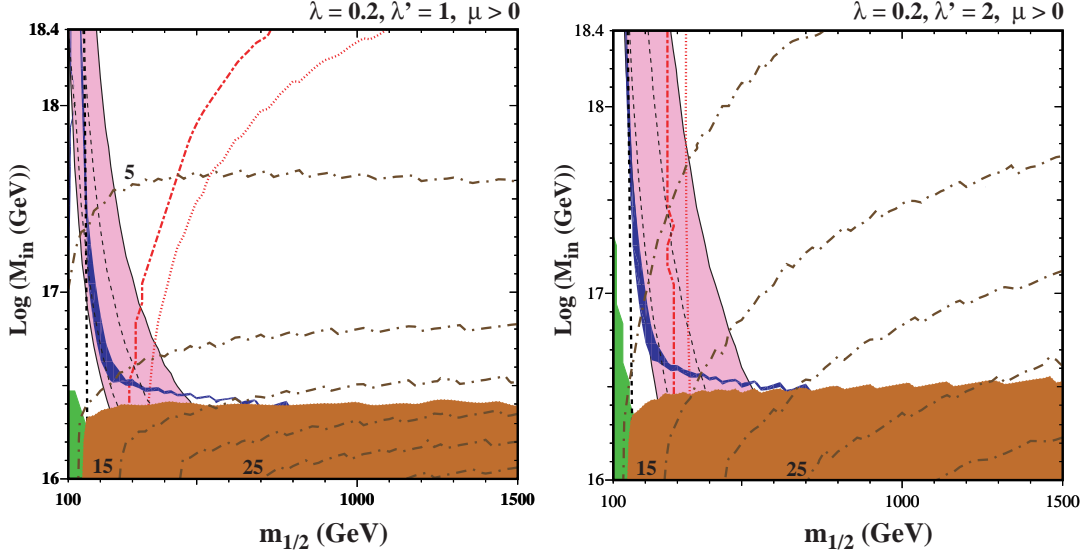


Figure 3: The $(m_{1/2}, M_{in})$ planes for $(\lambda, \lambda') = (0.2, 1)$ and $(0.2, 2)$ in the left and right plots, respectively. The curves and shadings have the same interpretations as for Fig. 1.

slopes of the $\tan\beta$ contours to decreasing positive values. That is, as $\lambda/\lambda' > 0$ increases, the right-hand side of eq. (18) decreases, and the $\tan\beta$ contours rotate clockwise, leading to smaller values of $\tan\beta$ for fixed $(m_{1/2}, M_{in})$. The region of parameter space allowed by the dark matter density constraint retains its L shape in this limit, with the base moving to lower M_{in} and the near-vertical arm to smaller $m_{1/2}$, as seen for the examples $(\lambda, \lambda') = (0.2, 1)$ and $(0.2, 2)$ shown in the left and right plots of Fig. 3, respectively. Because the vertical strip is situated at relatively low $\tan\beta$, it is excluded by the LEP Higgs mass constraint in both examples shown.

Fig. 4 displays the extensions of these results to the $(m_{1/2}, \lambda)$ planes for the fixed values $M_{in} = 10^{17}$ GeV (upper plots) and $M_{in} = \overline{M}_P$ (lower plots), for $\lambda' = 1$ (left plots) and $\lambda' = 2$ (right plots). We see that for $M_{in} = 10^{17}$ GeV and $\lambda' = 1$ the WMAP-compatible strip has $\lambda \sim -0.04$, whereas values of $-\lambda$ about twice as large are required if $\lambda' = 2$. A similar change in λ is seen in the lower plots for $M_{in} = \overline{M}_P$. On the other hand, the required values of λ do not change greatly between the two values of M_{in} . These plots therefore confirm the earlier finding that consistent no-scale models require $\lambda \ll \lambda'$, whatever the assumed values of λ' and $M_{in} \gg M_{GUT}$, and that the results are more sensitive to λ than to λ' . If extended to positive values of λ/λ' for these values of M_{in} , these plots would show a continuation of the vertical relic density strips at low $m_{1/2}$ which are excluded by the Higgs mass constraint. As M_{in} is lowered further (below 10^{17} GeV), the horizontal part of the L moves towards and into the positive λ/λ' domain.

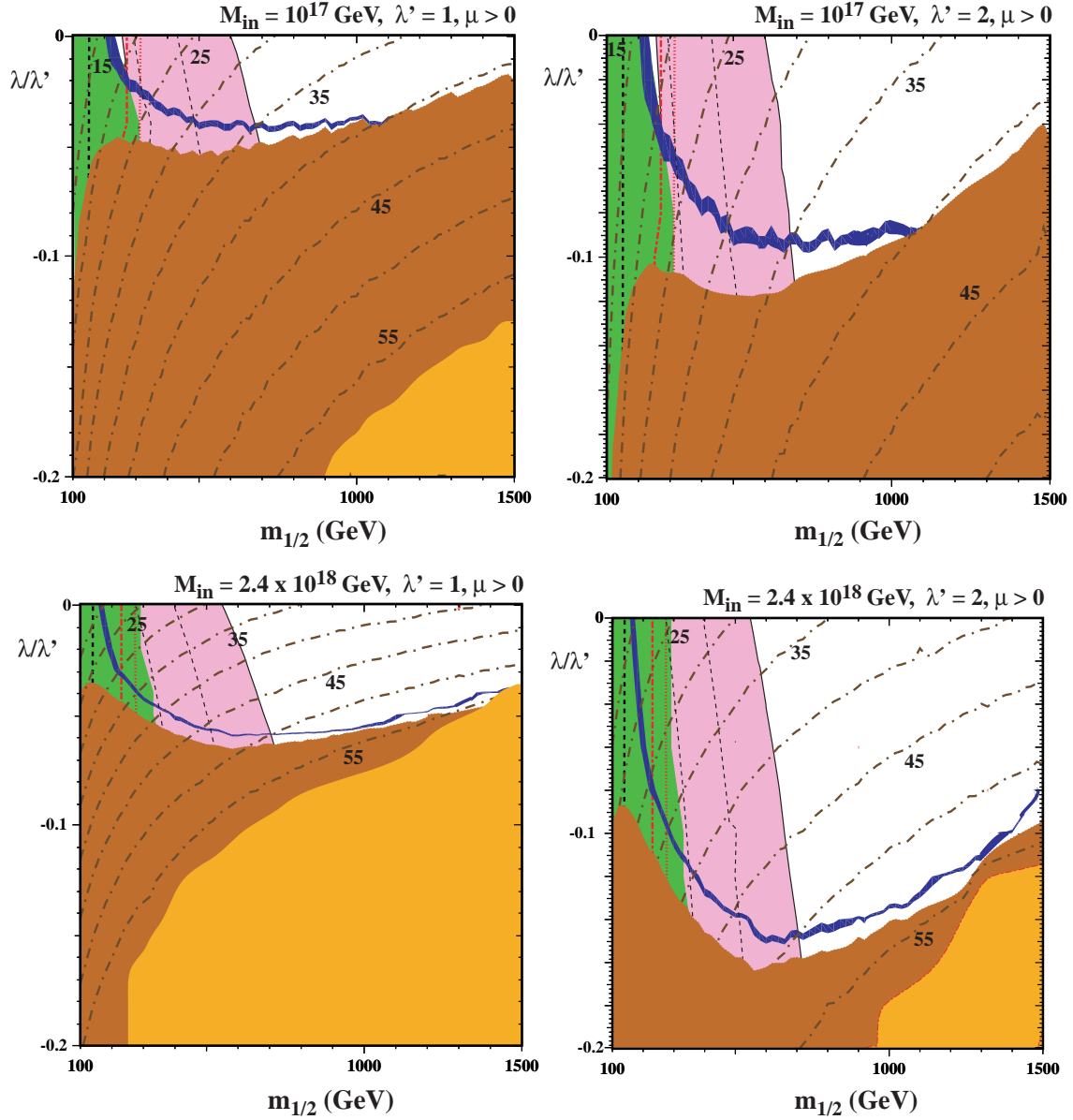


Figure 4: *The $(m_{1/2}, \lambda)$ planes for $M_{in} = 10^{17}$ GeV (upper plots) and $M_{in} = \overline{M}_P$ (lower plots), for $\lambda' = 1$ (left plots) and $\lambda' = 2$ (right plots). The curves and shadings have the same interpretations as for Fig. 1.*

4 Sparticle Spectra in No-Scale Models

Many of the features in Figs. 1 and 2 can be understood by looking at the sparticle spectra. In Fig. 5, we show how it changes with M_{in} for the specific choices $m_{1/2} = 700$ GeV, $\lambda' = 1$ and (left) $\lambda = -0.04$, (right) $\lambda = -0.06$ ⁸. We see in the left panel that the lighter stau, $\tilde{\tau}_1$, is the LSP and is lighter than the lightest neutralino, χ , for $M_{in} \lesssim 8 \times 10^{16}$ GeV, but increases monotonically in mass while m_χ remains roughly constant as M_{in} increases. The near-horizontal part of the WMAP-compatible strip in panel (b) of Fig 1 appears due to stau- χ coannihilation [48], which is important when the stau is only slightly heavier than the χ , for $M_{in} \sim 10^{17}$ GeV.

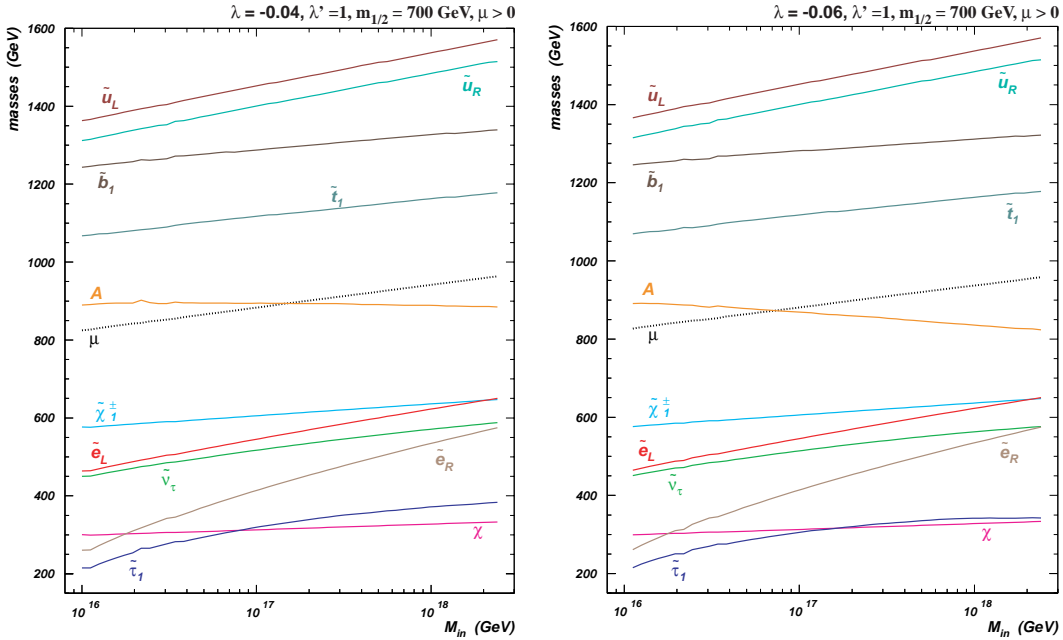


Figure 5: *The spectra in the no-scale $SU(5)$ model for $\lambda' = 1$ and $m_{1/2} = 700$ GeV and (left) $\lambda = -0.04$ and (right) $\lambda = -0.06$, as functions of M_{in} . Note that in each case there is an unacceptable range of low M_{in} where $m_{\tilde{\tau}_1} < m_\chi$, followed by range of higher M_{in} where $m_{\tilde{\tau}_1} > m_\chi$. There are viable coannihilation strips in the intermediate range of M_{in} near the crossing points.*

The evolution of the lighter stau mass with M_{in} is different in the right panel of Fig. 5, where $\lambda = -0.06$. We see that in this case, after crossing m_χ and rising further for low $M_{in} \lesssim 10^{18}$ GeV, the stau mass falls again for larger M_{in} . Here, there is a second region where stau- χ coannihilation is important and the relic density is brought within the WMAP range: one is just after the lower crossing point and the other is very close to $M_{in} = \overline{M}_P$. The base and hypotenuse of the WMAP triangles in panel (c) of Fig. 1 and panels (b) and (c) of Fig. 2 can be understood as these upper and lower coannihilation strips. Likewise, the

⁸Analogous plots for other values of $m_{1/2}$ and λ' show similar features.

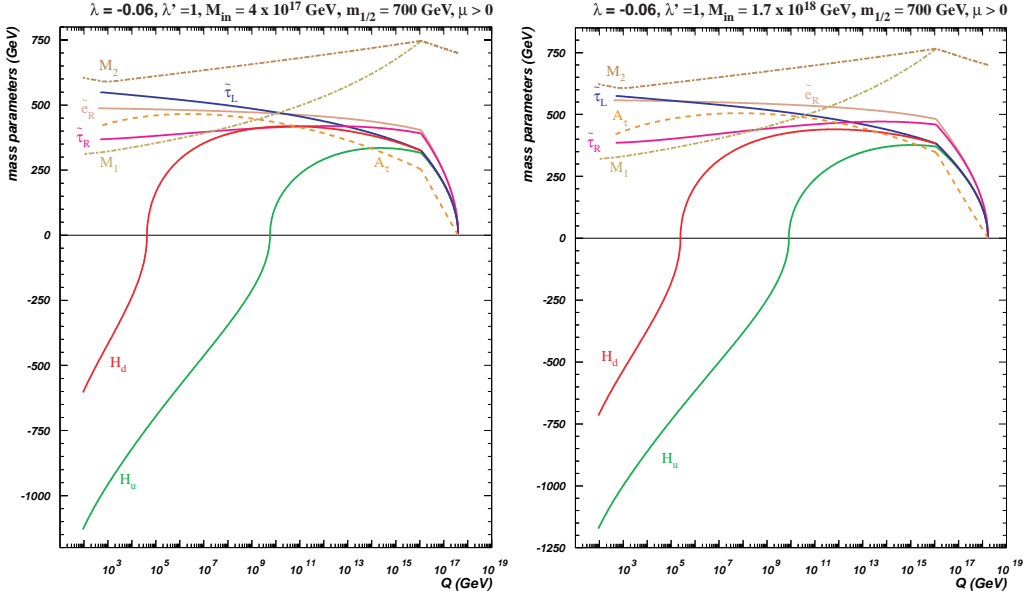


Figure 6: *The RG evolutions of the supersymmetry-breaking parameters in the no-scale $SU(5)$ model for $\lambda = -0.06$, $\lambda' = 1$ and $m_{1/2} = 700$ GeV, as a function of the renormalization scale Q , assuming $M_{in} = 4 \times 10^{17}$ GeV (left) and 1.7×10^{18} GeV (right). Note the rapid evolution of the trilinear parameter above M_{GUT} : the no-scale boundary condition at M_{in} leads to non-zero A_τ at M_{GUT} .*

doughnut in panel (d) of Fig. 1 and the blob in panel (d) of Fig. 2 can be understood as cases where the stau mass never rises much above m_χ so that the two coannihilation strips merge, and the disappearances of the doughnut and blob for larger values of λ are because the stau mass never rises (far enough) above m_χ . The same stau coannihilation mechanism operates in the nearly horizontal parts of Figs. 3 and 4.

These differences in the dependence of $m_{\tilde{\tau}_1}$ may be traced to the influence of the trilinear supersymmetry-breaking parameter A_τ . Specifically, the separation between $m_{\tilde{e}_R}$ and $m_{\tilde{\tau}_1}$ that increases with M_{in} , which is visible in both panels of Fig. 5, is due to A_τ . The growth of the separation with M_{in} reflects the rapid RG evolution of A_τ between M_{in} and the GUT scale seen in both panels of Fig. 6. As seen in (8), this evolution is sensitive to the value of λ , but not to λ' , except indirectly via the RGE for λ . In Fig. 6, we have assumed $\lambda = -0.06$: the effect of varying λ can be seen by comparing the left and right panels of Fig. 5. In the left panel with $\lambda = -0.04$, the separation between $m_{\tilde{e}_R}$ and $m_{\tilde{\tau}_1}$ is much smaller than in the right panel, where $\lambda = -0.06$ has been assumed, and the renormalization drives $m_{\tilde{\tau}_1}$ back close to m_χ at large M_{in} .

In the near-vertical part of the WMAP-allowed strips of Figs. 1 – 4, $\Omega_\chi h^2$ is lowered by a different mechanism. In this region, the $\tilde{\tau}_1$ is still the next-to-lightest supersymmetric particle but, due to the smallness of $m_{1/2}$, the $\tilde{\tau}_1 - \chi$ mass gap is too large for stau coannihilation to be effective. The smallness of $m_{1/2}$ also means that the soft supersymmetry-breaking scalar

masses are not pushed very high during the SU(5) evolution from M_{in} to M_{GUT} , resulting in a lighter sfermion spectrum. This in turn enables neutralinos to pair-annihilate efficiently into τ leptons via the exchange of staus in the t -channel – the same mechanism that operates in the bulk region of the CMSSM [4, 12]. Again just as in CMSSM, the light sfermion spectrum also leads to a light Higgs boson, creating tension with the LEP bound on m_h .

We also see in Fig. 5 that the mass of the CP-odd Higgs boson A decreases as M_{in} grows. This is because larger values of M_{in} lead to larger $\tan\beta$, as explained earlier. The larger value of $\tan\beta$ in turn produces a greater downward push of the H_d mass-squared parameter, resulting in a smaller value of $m_{H_d}^2$ at the weak scale, as can be seen in Fig. 6. Therefore the CP-odd Higgs boson mass, that is given at tree level by the expression $m_A^2 \simeq m_{H_d}^2 - m_{H_u}^2$, decreases as M_{in} increases. At some point it approaches $2m_\chi$, the condition necessary for the resonant pair annihilation via the direct Higgs channel [3, 5]. However, $m_{\tilde{\tau}_1}$ also decreases as M_{in} increases, and $\tilde{\tau}_1$ always becomes the LSP before the resonance condition $m_A \simeq 2m_\chi$ is reached. This can be traced to the dependence of $\tan\beta$ on $m_{1/2}$ in the no-scale scenario. Only if this dependence is broken as in Ref. [26, 31], where $\tan\beta$ is taken as a free parameter, can the A -funnel be reconciled with a framework with $m_0 = A_0 = 0$ and universal gaugino masses.

5 Sparticle Detection Prospects

We conclude by discussing the observability of sparticles in the no-scale models discussed here. We see from Figs. 1 and 2 that the portions of the WMAP-compatible no-scale strip that are also compatible with $g_\mu - 2$ at the 2- σ level have $250 \text{ GeV} \lesssim m_{1/2} \lesssim 700 \text{ GeV}$, compared with $m_{1/2} \lesssim 1500 \text{ GeV}$ if the $g_\mu - 2$ constraint is not applied. Since the only low-energy mass-scale is $m_{1/2}$, the low-energy spectrum is roughly proportional to $m_{1/2}$. Fig. 7 displays contours of $m_{\tilde{g}} = 500, 1000, 1500, 2000, 2500$ and 3000 GeV (blue dashed lines) for the choices $(\lambda, \lambda') = (-0.05, 1)$ (left plot) and $(-0.15, 2)$ (right plot)⁹. We see that $m_{\tilde{g}} \lesssim 1700 \text{ GeV}$ in the areas favoured by $g_\mu - 2$ at the 2- σ level, and may range up to $m_{\tilde{g}} \sim 2800 \text{ GeV}$ if the $g_\mu - 2$ constraint is discarded, still within the range of the LHC. We therefore conclude that the no-scale scenario is in principle testable in the near future. The spectra shown in Figs. 5 and 6 illustrate the range of possibilities for the sparticle masses for the case $m_{1/2} = 700 \text{ GeV}$, which is in the upper part of the possible range for $m_{1/2}$ if the $g_\mu - 2$ constraint is applied. We see that the heaviest squark may weigh up to $\sim 1350 \text{ GeV}$, while the gluino may weigh up to $\sim 1450 \text{ GeV}$: both of these are well within the reach of the LHC. Slepton masses range up to $\sim 500 \text{ GeV}$, within the reach of a 1-TeV linear collider.

Another approach to testing the no-scale model discussed here is through the direct detection of the LSP. Here, we follow the calculation outlined recently in [49] using $\Sigma_{\pi N} = 64 \text{ MeV}$: for details on the sensitivity to this choice, see [50]. Shown in Fig. 7 are contours of the spin-independent LSP dark matter scattering cross section $\sigma_{SI} = 10^{-8}$ and 10^{-9} pb (black solid lines - only the latter is visible in panel (b)). We see that values of $\sigma_{SI} \sim 10^{-8} \text{ pb}$ are typical, with a range extending less than an order of magnitude above and below if the $g_\mu - 2$

⁹The locations of these contours are relatively insensitive to the values of λ and λ' .

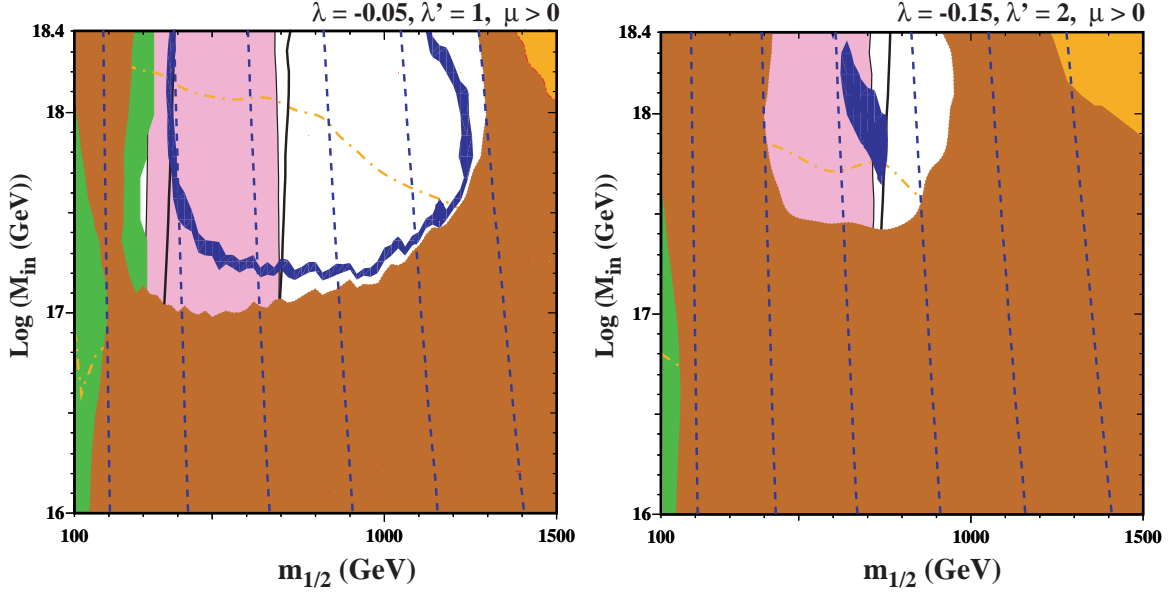


Figure 7: The $(m_{1/2}, M_{in})$ planes for $(\lambda, \lambda') = (-0.05, 1)$ and $(-0.15, 2)$ in the left and right plots, respectively, displaying contours of $m_{\tilde{g}} = 500, 1000, 1500, 2000, 2500$ and 3000 GeV (blue dashed lines), $\sigma_{SI} = 10^{-6}, 10^{-7}, 10^{-8}$ and 10^{-9} pb (black solid lines) and $h_b/h_\tau = 0.65$ and 0.6 (orange dashed lines). The other curves and shadings have the same interpretations as for Fig. 1.

constraint is applied, somewhat more if it is discarded. We also display in Fig. 7 contours of $h_b/h_\tau = 0.65$ and 0.6 as the lower and upper orange dashed lines, respectively. We see that these no-scale models violate $b-\tau$ Yukawa unification [51] quite significantly, pointing to the need either for higher-order non-renormalizable Yukawa couplings in the superpotential [52] or additional dynamics, e.g., in the neutrino sector [53], that might not affect other aspects of the analysis presented here.

In contrast, in the CMSSM the possible range of $m_{1/2}$ is larger, particularly in the focus-point region [54] and when there is rapid LSP-pair annihilation through the heavy Higgs bosons H, A in the direct channel [3, 5]. In both these regions, m_0 also takes large values, an impossibility in no-scale models. Because of these large values of $m_{1/2}$ and m_0 , the discovery of sparticles at the LHC cannot be guaranteed in the CMSSM¹⁰. It was to be expected that the range of experimental possibilities would be restricted in no-scale models: the good news is that the restriction is to accessible ranges of sparticle masses.

¹⁰The same is true in more general models such as the NUHM [11].

6 Acknowledgements

The work of A.M. and K.A.O. is supported in part by DOE grant DE-FG02-94ER-40823 at the University of Minnesota.

References

- [1] J. R. Ellis and D. V. Nanopoulos, Phys. Lett. B **110**, 44 (1982).
- [2] R. Barbieri and R. Gatto, Phys. Lett. B **110**, 211 (1982).
- [3] M. Drees and M. M. Nojiri, Phys. Rev. D **47** (1993) 376 [arXiv:hep-ph/9207234]; H. Baer and M. Brhlik, Phys. Rev. D **53** (1996) 597 [arXiv:hep-ph/9508321]; Phys. Rev. D **57** (1998) 567 [arXiv:hep-ph/9706509]; H. Baer, M. Brhlik, M. A. Diaz, J. Ferrandis, P. Mercadante, P. Quintana and X. Tata, Phys. Rev. D **63** (2001) 015007 [arXiv:hep-ph/0005027]; A. B. Lahanas, D. V. Nanopoulos and V. C. Spanos, Mod. Phys. Lett. A **16** (2001) 1229 [arXiv:hep-ph/0009065]; A. B. Lahanas and V. C. Spanos, Eur. Phys. J. C **23** (2002) 185 [arXiv:hep-ph/0106345].
- [4] J. R. Ellis, T. Falk, K. A. Olive and M. Schmitt, Phys. Lett. B **388** (1996) 97 [arXiv:hep-ph/9607292]; Phys. Lett. B **413** (1997) 355 [arXiv:hep-ph/9705444]; J. R. Ellis, T. Falk, G. Ganis, K. A. Olive and M. Schmitt, Phys. Rev. D **58** (1998) 095002 [arXiv:hep-ph/9801445]; V. D. Barger and C. Kao, Phys. Rev. D **57** (1998) 3131 [arXiv:hep-ph/9704403]. J. R. Ellis, T. Falk, G. Ganis and K. A. Olive, Phys. Rev. D **62** (2000) 075010 [arXiv:hep-ph/0004169].
- [5] J. R. Ellis, T. Falk, G. Ganis, K. A. Olive and M. Srednicki, Phys. Lett. B **510** (2001) 236 [arXiv:hep-ph/0102098].
- [6] V. D. Barger and C. Kao, Phys. Lett. B **518** (2001) 117 [arXiv:hep-ph/0106189]; L. Roszkowski, R. Ruiz de Austri and T. Nihei, JHEP **0108** (2001) 024 [arXiv:hep-ph/0106334]; A. Djouadi, M. Drees and J. L. Kneur, JHEP **0108** (2001) 055 [arXiv:hep-ph/0107316]; U. Chattopadhyay, A. Corsetti and P. Nath, Phys. Rev. D **66** (2002) 035003 [arXiv:hep-ph/0201001]; J. R. Ellis, K. A. Olive and Y. Santoso, New Jour. Phys. **4** (2002) 32 [arXiv:hep-ph/0202110]; H. Baer, C. Balazs, A. Belyaev, J. K. Mizukoshi, X. Tata and Y. Wang, JHEP **0207** (2002) 050 [arXiv:hep-ph/0205325]; R. L. Arnowitt and B. Dutta, arXiv:hep-ph/0211417.
- [7] J. R. Ellis, K. A. Olive, Y. Santoso and V. C. Spanos, Phys. Lett. B **565** (2003) 176 [arXiv:hep-ph/0303043]; H. Baer and C. Balazs, JCAP **0305**, 006 (2003) [arXiv:hep-ph/0303114]; A. B. Lahanas and D. V. Nanopoulos, Phys. Lett. B **568**, 55 (2003) [arXiv:hep-ph/0303130]; U. Chattopadhyay, A. Corsetti and P. Nath, Phys. Rev. D **68**, 035005 (2003) [arXiv:hep-ph/0303201]; C. Munoz, Int. J. Mod. Phys. A **19**, 3093 (2004) [arXiv:hep-ph/0309346].

- [8] J. R. Ellis, K. A. Olive, Y. Santoso and V. C. Spanos, Phys. Rev. D **69** (2004) 095004 [arXiv:hep-ph/0310356]; J. Ellis, S. Heinemeyer, K. Olive and G. Weiglein, *JHEP* **0502** 013, hep-ph/0411216; J. R. Ellis, S. Heinemeyer, K. A. Olive and G. Weiglein, *JHEP* **0605**, 005 (2006) [arXiv:hep-ph/0602220].
- [9] O. Buchmueller *et al.*, Phys. Lett. B **657** (2007) 87 [arXiv:0707.3447 [hep-ph]]; O. Buchmueller *et al.*, *JHEP* **0809** (2008) 117 [arXiv:0808.4128 [hep-ph]]; O. Buchmueller *et al.*, Eur. Phys. J. C **64**, 391 (2009) [arXiv:0907.5568 [hep-ph]].
- [10] D. Matalliotakis and H. P. Nilles, Nucl. Phys. B **435** (1995) 115 [arXiv:hep-ph/9407251]; M. Olechowski and S. Pokorski, Phys. Lett. B **344**, 201 (1995) [arXiv:hep-ph/9407404]; V. Berezinsky, A. Bottino, J. R. Ellis, N. Fornengo, G. Mignola and S. Scopel, Astropart. Phys. **5**, 1 (1996) [arXiv:hep-ph/9508249]; M. Drees, M. M. Nojiri, D. P. Roy and Y. Yamada, Phys. Rev. D **56**, 276 (1997) [Erratum-ibid. D **64** (1997) 039901] [arXiv:hep-ph/9701219]; M. Drees, Y. G. Kim, M. M. Nojiri, D. Toya, K. Hasuko and T. Kobayashi, Phys. Rev. D **63**, 035008 (2001) [arXiv:hep-ph/0007202]; P. Nath and R. Arnowitt, Phys. Rev. D **56**, 2820 (1997) [arXiv:hep-ph/9701301]; J. R. Ellis, T. Falk, G. Ganis, K. A. Olive and M. Schmitt, Phys. Rev. D **58**, 095002 (1998) [arXiv:hep-ph/9801445]; J. R. Ellis, T. Falk, G. Ganis and K. A. Olive, Phys. Rev. D **62** (2000) 075010 [arXiv:hep-ph/0004169]; A. Bottino, F. Donato, N. Fornengo and S. Scopel, Phys. Rev. D **63**, 125003 (2001) [arXiv:hep-ph/0010203]; D. Cerdeno and C. Munoz, *JHEP* **0410** (2004) 015, [arXiv:hep-ph/0405057].
- [11] J. Ellis, K. Olive and Y. Santoso, Phys. Lett. B **539**, 107 (2002) [arXiv:hep-ph/0204192]; J. R. Ellis, T. Falk, K. A. Olive and Y. Santoso, Nucl. Phys. B **652**, 259 (2003) [arXiv:hep-ph/0210205]; H. Baer, A. Mustafayev, S. Profumo, A. Belyaev and X. Tata, Phys. Rev. D **71**, 095008 (2005) [arXiv:hep-ph/0412059]. H. Baer, A. Mustafayev, S. Profumo, A. Belyaev and X. Tata, *JHEP* **0507** (2005) 065, [arXiv:hep-ph/0504001]; J. R. Ellis, K. A. Olive and P. Sandick, Phys. Rev. D **78**, 075012 (2008) [arXiv:0805.2343 [hep-ph]].
- [12] J. Ellis, J.S. Hagelin, D.V. Nanopoulos, K.A. Olive and M. Srednicki, Nucl. Phys. B **238** (1984) 453; see also H. Goldberg, Phys. Rev. Lett. **50** (1983) 1419.
- [13] J. Polonyi, *Generalization Of The Massive Scalar Multiplet Coupling To The Supergravity*, Hungary Central Inst Res - KFKI-77-93.
- [14] E. Cremmer, B. Julia, J. Scherk, P. van Nieuwenhuizen, S. Ferrara and L. Girardello, Phys. Lett. B **79**, 231 (1978); E. Cremmer, B. Julia, J. Scherk, S. Ferrara, L. Girardello and P. van Nieuwenhuizen, Nucl. Phys. B **147**, 105 (1979).
- [15] For reviews, see: H. P. Nilles, Phys. Rep. **110** (1984) 1; A. Brignole, L. E. Ibanez and C. Munoz, arXiv:hep-ph/9707209, published in *Perspectives on supersymmetry*, ed. G. L. Kane, pp. 125-148.
- [16] R. Barbieri, S. Ferrara and C. A. Savoy, Phys. Lett. B **119**, 343 (1982).

- [17] J. R. Ellis, K. A. Olive, Y. Santoso and V. C. Spanos, *Phys. Lett. B* **573** (2003) 162 [arXiv:hep-ph/0305212], and *Phys. Rev. D* **70** (2004) 055005 [arXiv:hep-ph/0405110].
- [18] L. E. Ibanez and G. G. Ross, *Phys. Lett. B* **110**, 215 (1982); L. E. Ibanez, *Phys. Lett. B* **118**, 73 (1982); J. R. Ellis, D. V. Nanopoulos and K. Tamvakis, *Phys. Lett. B* **121**, 123 (1983); L. Alvarez-Gaume, J. Polchinski and M. B. Wise, *Nucl. Phys. B* **221**, 495 (1983).
- [19] E. Cremmer, S. Ferrara, C. Kounnas and D. V. Nanopoulos, *Phys. Lett. B* **133**, 61 (1983); J. R. Ellis, C. Kounnas and D. V. Nanopoulos, *Nucl. Phys. B* **247**, 373 (1984).
- [20] E. Witten, *Phys. Lett. B* **155**, 151 (1985).
- [21] D. E. Kaplan, G. D. Kribs and M. Schmaltz, *Phys. Rev. D* **62**, 035010 (2000) [arXiv:hep-ph/9911293]; Z. Chacko, M. A. Luty, A. E. Nelson and E. Ponton, *JHEP* **0001**, 003 (2000) [arXiv:hep-ph/9911323].
- [22] J. R. Ellis, D. V. Nanopoulos and K. A. Olive, *Phys. Lett. B* **525**, 308 (2002) [arXiv:hep-ph/0109288].
- [23] H. Baer, C. Balazs, A. Belyaev, R. Dermisek, A. Mafi and A. Mustafayev, *JHEP* **0205**, 061 (2002) [arXiv:hep-ph/0204108].
- [24] M. Schmaltz and W. Skiba, *Phys. Rev. D* **62**, 095005 (2000) [arXiv:hep-ph/0001172].
- [25] M. Schmaltz and W. Skiba, *Phys. Rev. D* **62**, 095004 (2000) [arXiv:hep-ph/0004210].
- [26] J. Ellis, A. Mustafayev and K. A. Olive, arXiv:1003.3677 [hep-ph].
- [27] N. Polonsky and A. Pomarol, *Phys. Rev. Lett.* **73**, 2292 (1994) [arXiv:hep-ph/9406224], and *Phys. Rev. D* **51** (1995) 6532 [arXiv:hep-ph/9410231].
- [28] G. Senjanovic, arXiv:0912.5375 [hep-ph].
- [29] S. P. Martin and M. T. Vaughn, *Phys. Rev. D* **50** (1994) 2282 [arXiv:hep-ph/9311340].
- [30] A. Dedes, A. B. Lahanas and K. Tamvakis, *Phys. Rev. D* **53**, 3793 (1996) [arXiv:hep-ph/9504239].
- [31] H. Baer, M. A. Diaz, P. Quintana and X. Tata, *JHEP* **0004**, 016 (2000) [arXiv:hep-ph/0002245]; S. Profumo, *JHEP* **0306**, 052 (2003) [arXiv:hep-ph/0306119].
- [32] [The Muon g-2 Collaboration], *Phys. Rev. Lett.* **92** (2004) 161802, [arXiv:hep-ex/0401008]; G. Bennett et al. [The Muon g-2 Collaboration], *Phys. Rev. D* **73** (2006) 072003 [arXiv:hep-ex/0602035].

- [33] M. Davier, S. Eidelman, A. Hocker and Z. Zhang, *Eur. Phys. J. C* **31** (2003) 503 [arXiv:hep-ph/0308213]; M. Knecht, *Lect. Notes Phys.* **629**, 37 (2004) [arXiv:hep-ph/0307239]; K. Melnikov and A. Vainshtein, *Phys. Rev.* **D70** (2004) 113006 [arXiv:hep-ph/0312226]; J. F. de Troconiz and F. J. Yndurain, *Phys. Rev. D* **71**, 073008 (2005) [arXiv:hep-ph/0402285]; M. Passera, arXiv:hep-ph/0411168; K. Hagiwara, A. Martin, D. Nomura and T. Teubner, *Phys. Lett.* **B 649** (2007) 173 [arXiv:hep-ph/0611102]; M. Davier, *Nucl. Phys. Proc. Suppl.* **169**, 288 (2007) [arXiv:hep-ph/0701163]; F. Jegerlehner, *Acta Phys. Polon. B* **38**, 3021 (2007) [arXiv:hep-ph/0703125]; J. Miller, E. de Rafael and B. Roberts, *Rept. Prog. Phys.* **70** (2007) 795 [arXiv:hep-ph/0703049]; S. Eidelman, talk given at the ICHEP06, Moscow, July 2006, see:
http://ichep06.jinr.ru/reports/333_6s1_9p30_Eidelman.pdf
- [34] F. Borzumati and T. Yamashita, arXiv:0903.2793 [hep-ph].
- [35] L. J. Hall, J. D. Lykken and S. Weinberg, *Phys. Rev. D* **27**, 2359 (1983).
- [36] Information about this code is available from K. A. Olive: it contains important contributions from T. Falk, G. Ganis, A. Mustafayev, J. McDonald, K. A. Olive, P. Sandick, Y. Santoso and M. Srednicki.
- [37] ISAJET, by H. Baer, F. Paige, S. Protopopescu and X. Tata, arXiv:hep-ph/0312045.
- [38] Tevatron Electroweak Working Group and the CDF and D0 Collaborations, arXiv:0903.2503 [hep-ex].
- [39] C. Amsler *et al.* [Particle Data Group], *Phys. Lett. B* **667**, 1 (2008).
- [40] C. Degrandi, P. Gambino and G. F. Giudice, *JHEP* **0012** (2000) 009 [arXiv:hep-ph/0009337], as implemented by P. Gambino and G. Ganis.
- [41] J. R. Ellis, S. Heinemeyer, K. A. Olive, A. M. Weber and G. Weiglein, *JHEP* **0708**, 083 (2007) [arXiv:0706.0652 [hep-ph]].
- [42] E. Barberio *et al.* [Heavy Flavor Averaging Group (HFAG)], arXiv:hep-ex/0603003.
- [43] M. Davier, A. Hoecker, B. Malaescu, C. Z. Yuan and Z. Zhang, arXiv:0908.4300 [hep-ph].
- [44] Joint LEP 2 Supersymmetry Working Group, *Combined LEP Chargino Results up to 208 GeV*,
http://lepsusy.web.cern.ch/lepsusy/www/inos_moriond01/charginos_pub.html.
- [45] LEP Higgs Working Group for Higgs boson searches, OPAL Collaboration, ALEPH Collaboration, DELPHI Collaboration and L3 Collaboration, *Phys. Lett. B* **565** (2003) 61 [arXiv:hep-ex/0306033]. *Search for neutral Higgs bosons at LEP*, paper submitted to

ICHEP04, Beijing, LHWG-NOTE-2004-01, ALEPH-2004-008, DELPHI-2004-042, L3-NOTE-2820, OPAL-TN-744,
http://lephiggs.web.cern.ch/LEPHIGGS/papers/August2004_MSSM/index.html.

- [46] S. Heinemeyer, W. Hollik and G. Weiglein, *Comput. Phys. Commun.* **124** (2000) 76 [arXiv:hep-ph/9812320]; S. Heinemeyer, W. Hollik and G. Weiglein, *Eur. Phys. J. C* **9** (1999) 343 [arXiv:hep-ph/9812472].
- [47] J. Dunkley *et al.* [WMAP Collaboration], *Astrophys. J. Suppl.* **180**, 306 (2009) [arXiv:0803.0586 [astro-ph]]; E. Komatsu *et al.* [WMAP Collaboration], *Astrophys. J. Suppl.* **180**, 330 (2009) [arXiv:0803.0547 [astro-ph]].
- [48] J. R. Ellis, T. Falk and K. A. Olive, *Phys. Lett. B* **444** (1998) 367 [arXiv:hep-ph/9810360]; J. R. Ellis, T. Falk, K. A. Olive and M. Srednicki, *Astropart. Phys.* **13** (2000) 181 [Erratum-ibid. **15** (2001) 413] [arXiv:hep-ph/9905481]; R. Arnowitt, B. Dutta and Y. Santoso, *Nucl. Phys. B* **606** (2001) 59 [arXiv:hep-ph/0102181]; M. E. Gómez, G. Lazarides and C. Pallis, *Phys. Rev. D* **D61** (2000) 123512 [arXiv:hep-ph/9907261]; *Phys. Lett.* **B487** (2000) 313 [arXiv:hep-ph/0004028]; *Nucl. Phys. B* **B638** (2002) 165 [arXiv:hep-ph/0203131]; T. Nihei, L. Roszkowski and R. Ruiz de Austri, *JHEP* **0207** (2002) 024 [arXiv:hep-ph/0206266].
- [49] J. Ellis, K. A. Olive and P. Sandick, *New J. Phys.* **11**, 105015 (2009) [arXiv:0905.0107 [hep-ph]].
- [50] J. R. Ellis, K. A. Olive and C. Savage, *Phys. Rev. D* **77**, 065026 (2008) [arXiv:0801.3656 [hep-ph]].
- [51] M. S. Chanowitz, J. R. Ellis and M. K. Gaillard, *Nucl. Phys. B* **128**, 506 (1977); A. J. Buras, J. R. Ellis, M. K. Gaillard and D. V. Nanopoulos, *Nucl. Phys. B* **135**, 66 (1978).
- [52] See, for example: J. R. Ellis and M. K. Gaillard, *Phys. Lett. B* **88**, 315 (1979).
- [53] See, for example: M. S. Carena, J. R. Ellis, S. Lola and C. E. M. Wagner, *Eur. Phys. J. C* **12**, 507 (2000) [arXiv:hep-ph/9906362].
- [54] J. L. Feng, K. T. Matchev and T. Moroi, *Phys. Rev. Lett.* **84**, 2322 (2000) [arXiv:hep-ph/9908309], and *Phys. Rev. D* **61**, 075005 (2000) [arXiv:hep-ph/9909334]; J. L. Feng, K. T. Matchev and F. Wilczek, *Phys. Lett. B* **482**, 388 (2000) [arXiv:hep-ph/0004043].